

Dynamic Properties of RHA Steel under Planar Shock Loading using Explosive Driven Plate Impact System

B Venkataramudu^{*1}, P.C. Gautam[#], Ashish Paman['], V. Madhu['], and A.K. Gogia[']

¹Defence Metallurgical Research Laboratory, Hyderabad - 500 058, India

[#]Terminal Ballistics Research Laboratory, Chandigarh -160 030, India

^{*}E-mail: venkataramudub@dmrl.drdo.in

ABSTRACT

Planar shock loading of rolled homogeneous armour (RHA) steel has been studied at high pressures in the range of 20-100 GPa using an explosive-driven plate impact system. Shock velocities and flyer velocities are measured using time of arrival pins embedded in the target at known depths. The shock equation of state of RHA steel has been determined. $\alpha \rightarrow \epsilon$ phase transition stress and hughoniot elastic limit (HEL) of RHA steel have been determined through manganin gauge and found to be 12.2 ± 0.6 GPa and 4.1 ± 0.2 GPa, respectively. The experimental stress of phase transition has been compared with the stress calculated using ThermoCalc software. The shock properties have been incorporated in the Autodyn simulation package and simulations were performed to determine flyer velocity, pressures and the results are compared with that of experiments.

Keywords: Explosive-driven plate impact, hughoniot, RHA steel, time of arrival pins, manganin gauge, phase transition, Autodyn simulation software and ThermoCalc software

1. INTRODUCTION

The response of materials under high pressure shock loading has been extensively studied in the last few decades¹⁻². The plate impact is a widely used technique to understand the shock response such as HEL, phase transformation³⁻⁵, spall strength, and equation of state in materials. The principle of plate impact test lies in the generation of planar shock wave in target plates, due to the impact of flyer plate. The flyer plate can be accelerated either by explosive-driven⁶⁻⁷ or by a gas-driven⁸ mechanism. The leading edge of the shock wave, called shock front is generally defined as a discontinuity in pressure, density, and internal energy of the material at the interface between shocked and unshocked regions. Mass, momentum, and energy are conserved on both sides of the shock front. The corresponding conservation equations are called Rankine-Hugoniot jump conditions⁹. The relation between shock velocity (U) and particle velocity (u) is linear for most of the materials³ as shown below.

$$U = C_p + su \quad (1)$$

where the constant C_p , is the speed of sound in material at zero pressure, and s , is the material constant. The relation is said to be the shock equation of state of the material.

Shock properties and phase transitions in steel materials have been extensively studied using plate impact test¹⁰⁻¹¹. Weirik¹⁰ has studied phase transformations of 4340 steels using light gas gun and found that phase transition occur at 13 GPa. Martin¹¹, *et al.* have investigated the phase transformation of eglin steel using gas-driven impact test and VISAR diagnostic and found to occur at 12.8 GPa. However no studies on shock

behaviour and phase transformation of rolled homogenous steel using explosive-driven plate impact system have been reported. RHA steel is one of the important and extensively used armour materials due to its high strength and energy-absorbing capability. Therefore, it is very important to understand the shock behaviour and phase transformations under high pressure shock loading.

The objective of the study is to generate equation of state and stress-time history profile in the pressure range of 20 GPa - 100 GPa using explosive-driven plate impact. The HEL and phase transformation stresses are also determined in this study. The phase transformation stress, determined by plate impact tests, was compared, with the stress calculated using thermoCalc software. The comparison of flyer velocity and hughoniot pressures determined by both experiments and simulated results using Autodyn package is also presented.

2. EXPERIMENTAL SETUP

The plate impact experiments were carried out using 200 mm diameter explosive-driven plate impact test set up at Terminal Ballistics Research Laboratory (TBRL), Chandigarh. The typical test setup is shown Fig.1. The system consists of a detonator, plane wave shaper (PWS), high explosive pad, flyer plate, and target plates. The PWS is in the form of hollow cone prepared using RDX/TNT explosive having high velocity of detonation (VoD). The cone is filled with Baratol explosive of low VoD. The cone angle of the PWS is 41° which depends on VoDs of both the explosives. The PWS is followed by high explosive (HE) RDX/TNT Pad. The pad thickness was varied

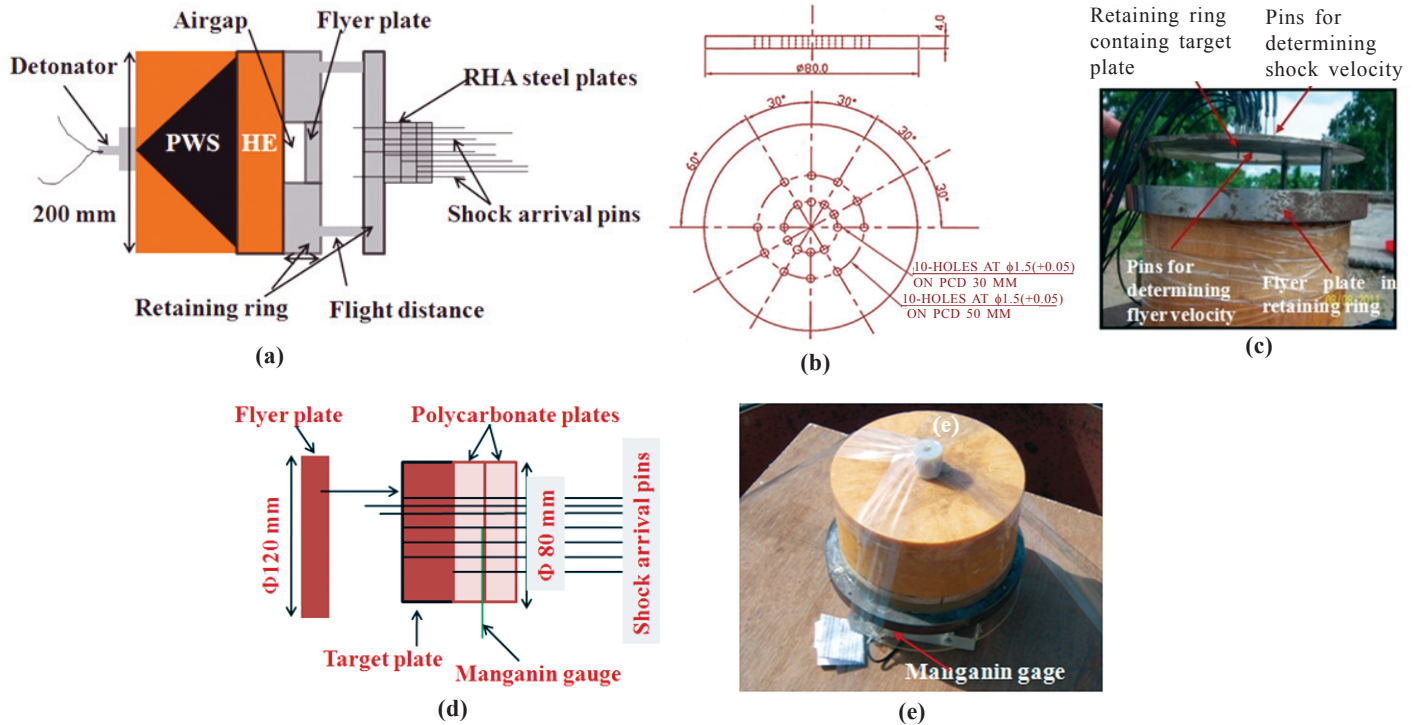


Figure 1. Experimental setup (a) Schematic drawing with pins, (b) Shock arrival pin arrangement in the target material (backside view), (c) Top view, (d) Schematic drawing with pins and manganin gauge, and (e) Experiment with manganin gauge.

from 10 mm to 100 mm to achieve required flyer velocities. Subsequently, an air gap of about 5 mm - 10 mm is maintained between HE pad and flyer plate to ensure uniform expansion of explosive gases. Flyer plate is held tightly by the retaining rings. SS-304 flyer plates of 120 mm diameter with different thicknesses ranging from 5 mm to 15 mm were used in the experiments. A flight of 25 mm - 50 mm has to be traversed by the flyer plate to attain maximum velocity before hitting the target plates. The target plates of 80 mm diameter and 4 mm thick RHA discs were clamped to the retaining ring.

The detonator is used to initiate PWS. The shock wave emanating from the PWS is planar, which in turn initiates the HE pad to form a high pressure planar shock wave. The shock wave propels the flyer plate to required velocities depending on the thickness of the HE pad. After attaining maximum velocity, the flyer plate hits the target plate normally. This impact generates planar shock wave both in target and flyer plates. The characteristics of shock wave in target plate are measured by deploying shorting pins and manganin gauges.

The arrangement of shock arrival pins¹²⁻¹⁴ at different locations in the target is shown in Fig. 1(b). The photograph of the target with shock arrival pins is shown in Fig. 1(c). The pins were connected to pin mixer and subsequently to

data acquisition system of 1GS/s sampling rate. In one of the experiments, a manganin gauge was used to record stress-time history profile of the shock propagation in the RHA target plate. The gauge was embedded between two polycarbonate plates (PC) of 5 mm thickness after steel target plate, as shown in Fig. 1(d) schematically and Fig. 1(e) experimentally. The polycarbonate plates were used to protect the gauge from damage before the shock traverses the gauge. The gauge was connected to pulse power supply unit. The voltage–time history data was recorded using a 10 GS/s oscilloscope. The voltage-time data was reduced to stress–time history in PC following Rosenberg’s work¹⁵.

3. MATERIAL DESCRIPTION

RHA steel as received was used in all the experiments. The chemical composition and mechanical properties of RHA steel are shown in Table 1 and Table 2. All the samples used for plate impact experiments were taken from a single large plate to ensure uniformity. 80mm diameter and 4mm thick samples in the disc form were cut from the single large plate using wire cut electro-discharge machining (EDM) machine. Subsequently the disc samples were milled and lapped to precise dimensions. 1.2 mm diameter holes are drilled through the sample to deploy

Table 1. Chemical composition of RHA steel

Element	C	Si	Ni	Mn	Cr	V	Mo	Al	Fe
(Wt. per cent)	0.3-0.35	0.2-0.3	1.5-2.0	0.5-0.7	1.4-1.7	0.1-0.2	0.3-0.5	0.02	Bal.

Table 2. Mechanical and ultrasonic properties of RHA steel

ρ (g/cc)	C_L (m/s)	C_S (m/s)	C_B (m/s)	El (per cent)	YS (MPa)	UTS (MPa)	Hardness (VHN)
7.85	5910	3930	3786	16	1080	1250	320

shorting pins. The planarity of < 1 μm and surface finish of < 25 μm was maintained to minimise the errors due to inertia and friction. Ultrasonic measurements such as longitudinal and shear sound speeds, were determined on five samples and average values are tabulated in Table 2.

Shorting pins, manganin gauges and related equipment used were manufactured by M/s. Dynasen Inc., USA. Real-time measurements were recorded using Agilent data acquisition system and Tektronix digital oscilloscope.

4. NUMERICAL MODELLING AND SIMULATION

4.1 Autodyn Simulations

Finite element modelling and simulation of explosive-driven plate impact was performed using Autodyn¹⁶ dynamic explicit analysis package. The simulation of explosive-driven plate impact system provides knowledge of interface pressure, particle velocity, shock velocity, and stress-time history profiles in the material. The basic objective of the simulation is to determine flyer velocities and hugoniot stresses and to compare with experimental results. The entire material model is described with air, Baratol, RDX/TNT, SS-304 for flyer and retaining rings and RHA steel for target plates. For simplicity axi-symmetric modelling was employed. The entire continuum is discretized using hexahedral element with aspect ratio of one. Euler lagrangian processor is used for solving the problem. In the simulation, air is modelled using Eulerian grid and remaining parts are modelled using Langrangian grid. Flow out boundary condition is given for air as it is free to expand whereas fixed-boundary conditions are given for retaining rings by making all translations and rotations as zero. All the boundary conditions including loading parameters were taken in line with experimental parameters. These parameters are detailed at Table 3.

From simulation, the flyer velocities and hugoniot stresses are determined and compared with corresponding experimental values. To determine the above results through simulation, parameters for a rate-dependent material model, equation of state, and failure model are essential.

The Johnson-Cook strength model for the RHA steel is used to determine flow stress (σ) of the material as a function of plastic strain (ε), strain rate (ε̇), and relative temperature (T^{*}).

$$\sigma = (A + B \epsilon^n)(1 - C \ln \dot{\epsilon})(1 + T^{*m}) \tag{2}$$

The parameters *A*, *B*, *C*, *m* and *n* are determined from quasi-static and high-strain rate tests. The equation of state parameters (*C_p*, *s*), are taken from present work¹⁷. The parameters of strength model and equation of state used for RHA steel are tabulated in Table 5. A plastic strain value of 0.5 is used such that the elements, which are stressed above this value can be discarded from calculation. The explosives Baratol and R/T pad become gaseous once these are initiated. Hence the explosives are modelled using JWL equation of state and material parameters were directly taken from Autodyn material library.

4.2 Thermo-Calc Calculations

ThermoCalc software is based on thermodynamic relations. The software works on materials database of free energy functions, free energy data from electronic structures. etc. The software gives various types of outputs like, phase predominance diagrams, multi-component phase diagrams and phase fractions, etc. The first stage of the flow chart of a project in ThermoCalc software is to define number of elements, their phase constituents and chemical composition. Second is to define an equilibrium calculator mentioning the values of axes and their corresponding ranges. Third is to draw a plot of various phases. In the present work, in-built TCFE5 database, of iron and other constituent elements of steel is used to obtain pressure-temperature phase diagram for RHA steel.

5. RESULTS AND DISCUSSION

5.1 Shock Hugoniot Data

The flyer plate was accelerated by the planar shock wave, generated by the detonation of HE Pad. The velocity of the flyer plate was measured using self-shortening pins located in the air gap at various distances. The shock velocities in the target material were also measured using self-shortening pins located at various depths in the target. Typical voltage–time plot showing arrival times at various pin depths are shown in Fig. 2. The average of arrival times of flyer plate and shock waves at different locations were recorded and shown in Figs 3 (a) and 3(b), respectively. The inverse of slopes of the above graphs were calculated to determine flyer and shock velocities and tabulated at Table 4. By using impedance matching condition

and Rankine–Hugoniot (RH) equations, particle velocity and pressure in target material were calculated and tabulated at Table 4. The SS-304 (flyer) hugoniot between particle velocity and shock velocity is used during above calculations¹⁸ and is given by

$$U = 4.570 + 1.49 u \tag{3}$$

The hugoniot curve between particle velocity and pressure is shown in Fig. 4(a). The hugoniot curve between particle velocity and shock velocity is shown in Fig. 4(b). The curves are compared with hugoniot curves of ε- phase and α- phase RHA steel reported by Franz and Robitaille¹⁹. From Fig. 4(a), it is evident that the present experimental

Table 3. Impact conditions of experiments

Parameter / Experiments	Expt. 1	Expt. 2	Expt. 3	Expt. 4	Expt. 5 [#]	
PWS	Thickness (mm)	88	90	88	89	90
	Diameter (mm)	200	200	200	200	200
HE-RDX / TNT	Thickness (mm)	0	55	60	100	0
	Diameter (mm)	0	200	200	200	0
Flyer-SS-304	Thickness (mm)	15	10	5	5	15
	Diameter (mm)	120	120	120	120	120
Target–Steel (4Nos.)	Thickness (mm)	16.1	15.8	16.2	15.9	10
	Diameter (mm)	80	80	80	80	80
	Airgap (mm)	6.2	9.0	7.0	2.5	6.2
	Flight (mm)	20	29	25	45	20

[#]Manganin gauge experiment

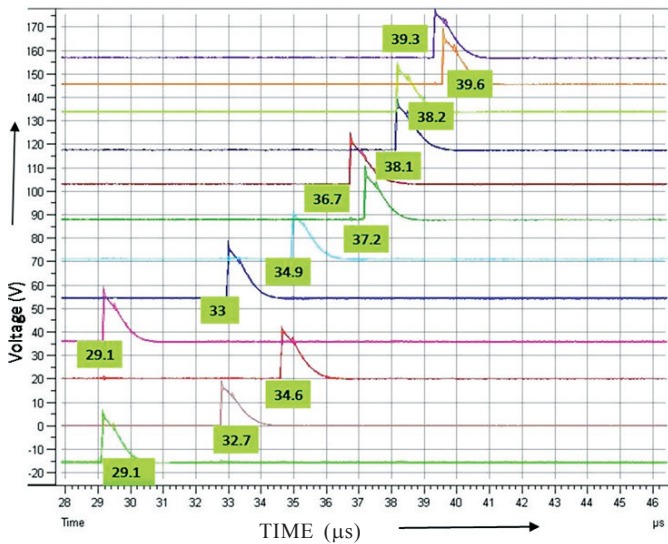


Figure 2. Experimental voltage-time graph showing shock arrival times at various pin depths in target, for flyer velocity of 1085 m/s.

results are close to ϵ - phase RHA steel despite the difference in mechanical properties, composition and heat treatment. From Fig. 4(b), it is observed that with the increase in particle velocity, shock velocity also increases linearly. The Hugoniot between the particle velocity and shock velocity is represented by the following linear fitting equation.

$$U = 4.301 + 1.153 u \tag{4}$$

where C_0 is 4.301 km/s and s is 1.153. These parameters are used in hydrodynamic modelling of the material in Autodyn software package.

5.2 Phase Transition Data

As the shock wave is travelling from high-shock impedance RHA target to low-shock impedance PC material, it gets reflected as a rarefaction wave into the RHA target and travels as a weak shock wave into the polycarbonate material. Therefore, the stress in the target plate was measured indirectly by measuring the stress in the polycarbonate plates which are attached to the back side of the target plate. The stress (σ) at different times in the PC material was measured using manganin gauge and calculated by following equation¹⁵

$$\sigma = k \frac{\Delta R}{R} \tag{5}$$

where k is 0.4 GPa for the manganin gauge and $\frac{\Delta R}{R}$ is relative

Table 4. Experimental results for un-symmetric flyer impact of RHA steel material

Parameters / Experiment No.	Flyer velocity (m/s)	Shock velocity (m/s)	Particle velocity (m/s)	Pressure (GPa)	Flyer ‡ velocity (m/s)	Pressure ‡ (GPa)
Expt.1	1198	4463	656	22.98	1200	23.9
Expt.2	2010	5387	1061	44.87	1800	43.6
Expt.3	2797	6058	1459	69.38	2400	61.5
Expt.4	3540	6667	1853	95.93	3000	75.6
Expt.5	1085	4600	627	22.64	1200	23.9

‡Simulation results

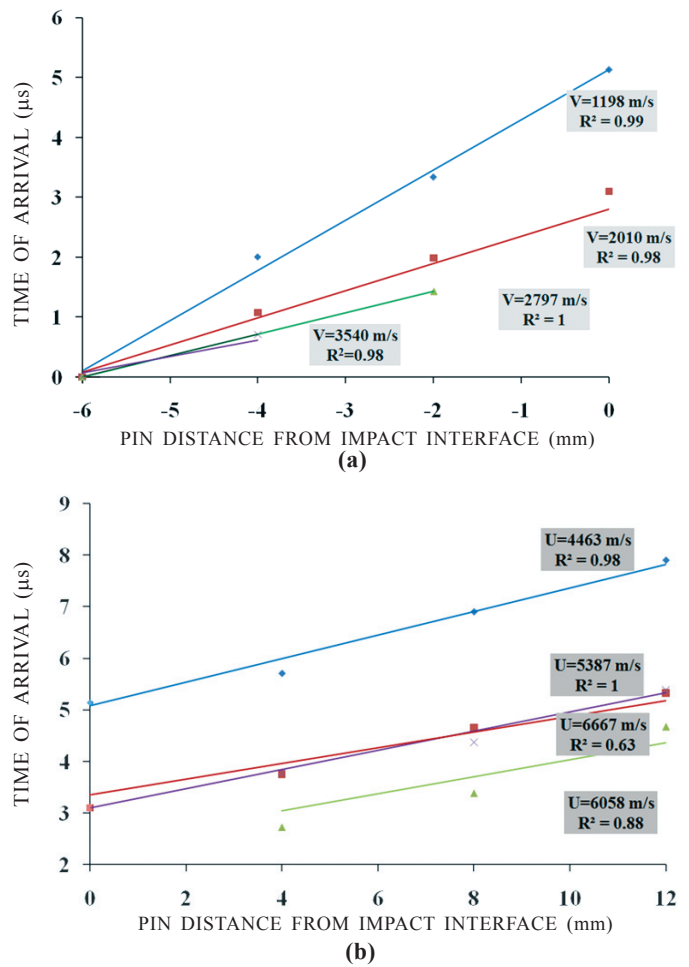


Figure 3. (a) Determination of flyer velocity from pins in air (b) Determination of shock velocity from pins in material.

change of resistance of the manganin gauge. Then the particle velocities in the PC materials and at steel-PC interface were calculated using RH equations and impedance-matching conditions²⁰. The particle velocity at the interface was used in the calculation of stress in the RHA target. The stress - time history profile thus determined is shown in Fig. 5. It

Table 5. Material parameters of RHA steel used in Autodyn for modelling and simulation of the experiments

ρ (g/cc)	A (MPa)	B (MPa)	C	n	m	γ_0	C_0 (km/s)	s
7.85	1320	975	0.82	0.0417	1	1.67	4.301	1.153

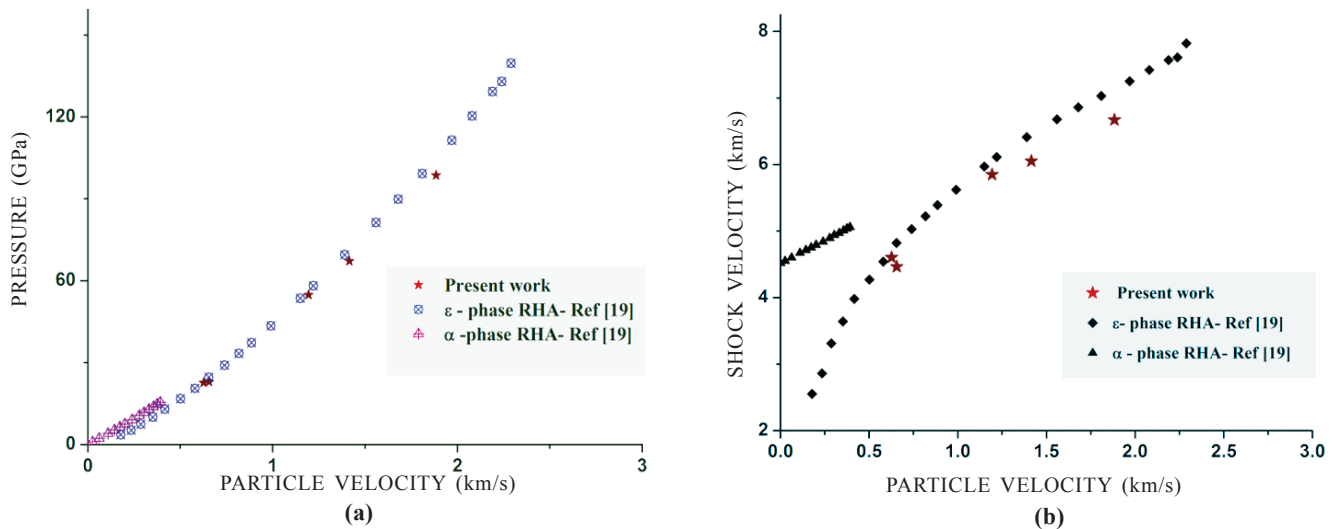


Figure 4. Hugoniot curves for steel material : (a) Pressure –particle velocity, and (b) Shock velocity - particle velocity.

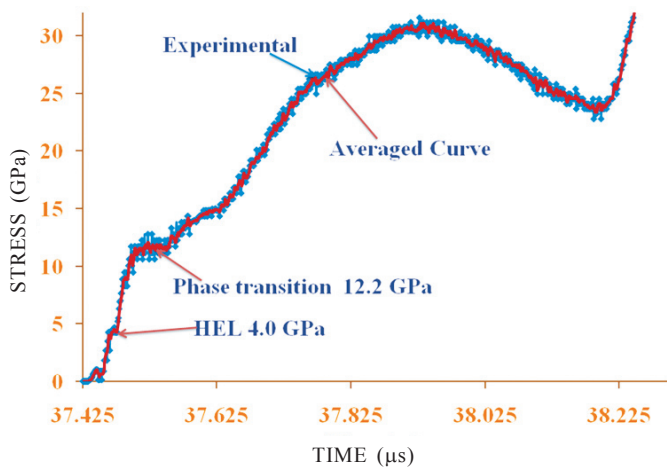


Figure 5. Stress-time history profile showing HEL and phase transformation in RHA steel at a flyer velocity of 1085 m/s.

is observed from the profile that an elastic wave started to appear at 37.43 μs after detonator is triggered. The limit of the elastic wave is called hugoniot elastic limit (HEL) and found to be 4.1 ± 0.2 GPa. Immediately after the elastic shock, plastic waves started growing. After 0.05 μs, phase transition waves were initiated at a planar shock compression of 12.2 ± 0.5 GPa. The phase transition waves gradually increase to hugoniot pressure of 30 GPa in a time gap of 0.42 μs. Hence, from Fig. 5, onset of phase transition is at a stress of 12.2 ± 0.5 GPa which is compared with the results of ThermoCalc software.

5.3 Analysis of Phase Transition with ThermoCalc

The phase transformation in this steel has been analysed with ThermoCalc software. Pressure – Temperature phase diagram of pure iron has been generated. The P-T diagrams of pure iron, iron with 0.3 wt per cent carbon, and RHA steel are generated and shown in Fig. 6. From the figure, it is observed that pure iron exhibits α (BCC) \rightarrow ϵ (HCP) phase transition point at 13.1 GPa, however this phase transition stress has

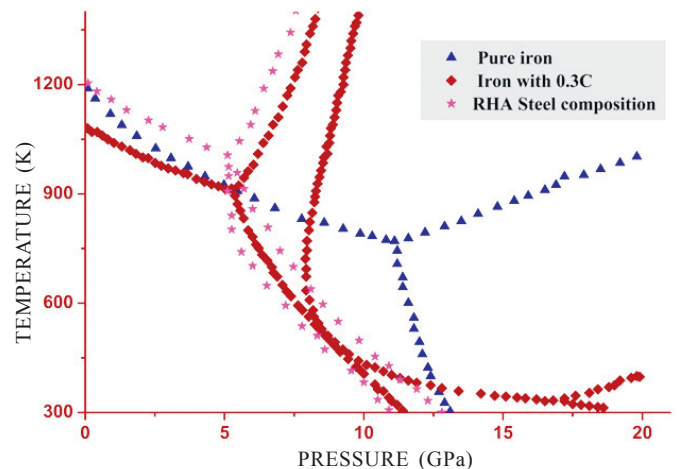


Figure 6. Comparison of P-T diagram of Iron, Fe-0.3 percent C and RHA steel composition calculated using ThermoCalc.

decreased to 12.1 GPa with addition of 0.3 Wt. per cent of carbon to pure iron. RHA steel which consists of iron 0.3 per cent carbon and other elements has exhibited α (BCC) \rightarrow ϵ (HCP) phase transition at 12.0 ± 0.6 GPa. From the above it is evident that there is no significant effect of constituent elements other than 0.3 Wt. per cent of carbon in the pressure-induced phase transition of RHA steel. It is also observed that with the increase in the temperature of the material, α (BCC) \rightarrow ϵ (HCP), phase transition stress decreases. The phase transition stress obtained through ThermoCalc analysis is matching with experimental results.

5.4 Simulation of Explosive-Driven Plate Impact Test

Simulations were carried out at different parameters mentioned in Table 3 and the corresponding flyer velocities and shock pressures in RHA target were determined. Typical simulated model for a flyer velocity of 3000 m/s at zero cycle and 1700 cycles is shown in Figs 7 (a) and 7(b), respectively. From the Fig. 7 (a), no shock formation or flyer movement was

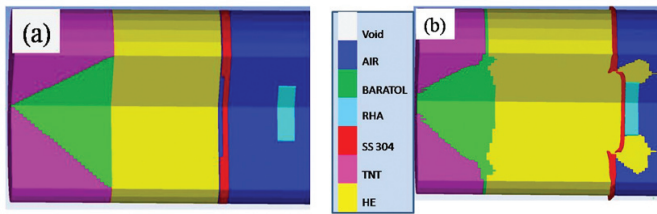


Figure 7. Modelling of explosive-driven plate impact 270° view at HE of 100 mm thick (a) at 0 cycle, and (b) Impact of flyer plate with target plate at 1700 cycle.

observed as detonation has not been initiated, whereas Fig. 7(b) shows the shock initiation at the flyer target interface during impact and propagation of planar shock wave in the flyer and target plates. The flyer velocity - time history and pressure - time history profiles have been captured by introducing gauge points in the target plates. Both the experimental and simulated flyer velocities and hughoniot pressures are compared and shown in Fig. 8 and Table 4. The simulation results are matching with experimental results within the range of 10-20 per cent error. Both from the experiments and simulations, it is observed that the pressure increases with flyer velocity.

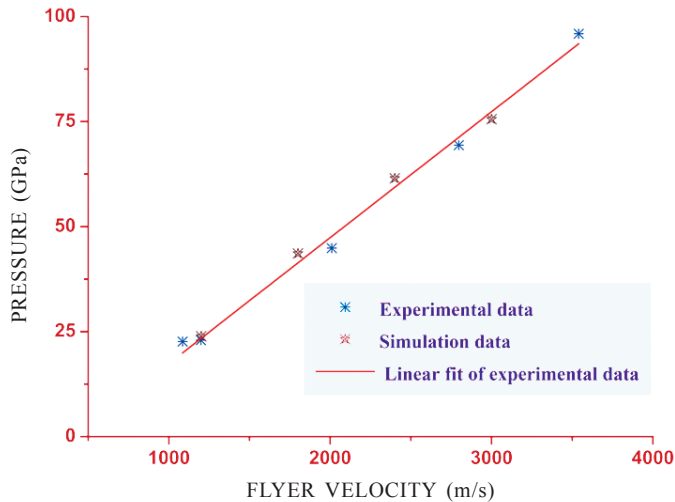


Figure 8. Comparison of experimental and simulated pressures and flyer velocities.

6. CONCLUSIONS

A series of experiments were carried out using Explosive driven plate impact system to determine various shock parameters like HEL, phase transition stress, hughoniot pressure, shock velocity, and particle velocity. From the experiments following conclusions are drawn.

- The hughoniot curve between shock velocity and particle velocity is used to generate linear shock equation of state of the material. The equation of state (EOS) is $U = 4.301 + 1.153 u$ for particle velocity range of 0.5 km/s to 2.0 km/s. The EOS parameters are used to model the hydrodynamic behaviour of the material.
- The pressure-particle velocity and shock velocity-particle velocity hughoniot curves are comparable with ϵ - phase RHA steel.
- Manganin stress gauge was used to capture the stress - time history of the material under a planar shock wave of

30 GPa pressure. The stress - time history profile was used to determine HEL, phase transition stress of the material and are found to be 4.1 ± 0.2 GPa and 12.2 ± 0.5 GPa, respectively.

- ThermoCalc software was used to determine the phase transition stress and is matching with the experimental stress.
- The Finite element simulations of explosive-driven plate impact were carried out successfully to compare the experimental flyer velocities and hughoniot pressures. The results are found to be in good agreement with the experimental results.

REFERENCES

1. Bourne, N.K.; Gray, G.T. & Millet, J.C.F. On the shock response of cubic metals. *J. Appl. Phys.*, 2009, **106**, 091301. doi: 10.1063/1.3218758
2. Bourne, N.K. & Millet, J. Contrasting the shock properties of iron and a steel. *Scripta Mater.*, 2000, **43**, 541. doi: 10.1016/S1359-6462(00)00429-2
3. Barker, L.M. & Hollenbach, R.E. Shock wave study of the $\alpha \rightleftharpoons \epsilon$ phase transition in iron. *J. Appl. Phys.*, 1974, **45**, 4872. doi: 10.1063/1.1663148
4. Bancroft, D.; Peterson, E.L. & Minshall, S. Polymorphism of iron at high pressure. *J. Appl. Phys.*, 1956, **27**, 291. doi: 10.1063/1.1722359
5. Martin, B.E.; Flater, P.J.; Abrahams, R.A.; Neel, C.H.; Reinhart, W.D. & Chhabildas, L.C. Dynamic characterization of eglin steel by symmetric impact experimentation. *AIP Conf. Proc.*, 2012, 1426, 979. doi: 10.1063/1.3686441
6. Singh, Manjit. Explosive laboratory devices for dynamic shock loading of materials in mbar pressure region. *J. Phy. Conf. Series*, 2012, **377**, 012003. doi: 10.1088/1742-6596/377/1/012003
7. Mcqueen, R.G. & Marsh, S.P. Equation of state for nineteen metallic elements from shock-wave measurements to two megabars. *J. Appl. Phys.*, 1950, **31**, 1253. doi: 10.1063/1.1735815
8. Zhernokletov, M.V. & Glushak, B.L. Material properties under intensive dynamic loading. Springer, 2006, USA, pp.33. doi: 10.1007/978-3-540-36845-8
9. Meyers, M.A. Dynamic behaviour of materials. Wiley Interscience, USA, 1994, pp.98 doi: 10.1002/9780470172278
10. Weirick, L.J. Plane shock generator of explosive lens: shock characterization of 4340 and PH13-8Mo steels, c360 Brass and PZT 65/35 Ferro-Electric ceramic, SAND93-3919.UC-742. March 1994.
11. Martin, Bradley E.; Flater, Philip J.; Abrahams, Rachel A.; Neel, Christopher H.; Reinhart, William D. & Chhabildas, Lalit C. Dynamic characterization of Eglin steel by symmetric impact experimentation. *AIP Conf. Proc.* 2012, 1426, 979.
12. Wasley, Richard J.; O'Brien, Joseph F. & Henley, Darwin R. Design and construction of a new coaxial electrical discharge pin. *Rev. Sci. Instrum.*, 1964, **35**, 466. doi: 10.1063/1.1718847
13. Erskine, D.J. Improved arrangement of shock-detecting

- pins in shock equation of state experiments. *Rev. Sci. Instrum.*, 1995, **66**, 5032. doi: 10.1063/1.1146523
14. Minshall, S. Properties of elastic and plastic waves determined by pin contactors and crystals. *J. Appl. phys.*, 1995, , 463. doi: 10.1063/1.1722019
 15. Rosenberg, Z.; Yaziv, D. & Partom, Y. Calibration of foil-like manganin gauges in planar shock wave experiments. *J. Appl. Phys.*, 1980, **51**, 3702. doi: 10.1063/1.328155
 16. Autodyn software package, Century Dynamics Ltd.
 17. Venkataramudu, B.; Gautam, P.C.; Madhu, V. & Gogia, A.K. DRDO-DMRL-ADDG-II-044 – 2013. May 2013.
 18. Marsh, S.P. (ed.), LASL Shock hugoniot data. Univ. of California Press, CA, 1980, 212p.
 19. Franz, R.E. & Robitaille, J.L. The Hugoniot of 4340 Steel Rc 54-55, ARBRL-MR-02951. September 1979.
 20. Cooper, P.W. Explosive engineering. Wiley-VCH Publications, USA, 1996, pp.185.

ACKNOWLEDGEMENTS

The authors would like to thank Director, DMRL for giving permission to publish the present work and Director, TBRL for his constant support in performing the experiments. Authors would also like to thank, Armour Design and Development Division of DMRL and a team of TBRL personnel for machining works and conducting the plate impact experiments.

CONTRIBUTORS

Mr B. Venkataramudu has fabricated RHA target samples in required dimensions and evaluated the physical and mechanical properties of the material. He has also analyzed the data from the experiments and compared the results with Autodyn simulations. He has performed the Thermocalc calculations and results are compared with experiments. He also prepared the manuscript as per DSJ format.

Mr P.C. Gautam has performed the experiments at various flyer velocities varying the thickness of high explosive pad in explosive driven plate impact test setup.

Mr Ashish Paman has performed the Autodyn simulations from creating the model to simulate the setup completely and various simulation results like flyer velocity and pressure are calculated.

Dr Vemuri Madhu and **Dr A.K. Gogia** They have been involved in planning of work and arranging various materials and sensors required for experiments. They also verified and corrected the manuscript.